N.M. CHEPILKO, S.A. PONOMARENKO

Instutute of Aerospace Technologies,
National Technical University of Ukraine "Igor Sikorsky Kyiv Polytechnic Institute"
(37, Beresteiskyi Ave., Kyiv 03056, Ukraine; e-mail: chepilkonm@gmail.com)

PHYSICAL PRINCIPLES OF A FERROMAGNETIC GYROSCOPE WITH NANOSCALE SENSITIVE ELEMENTS

Physical principles of applying modern nanotechnologies to develop nano-sized and energy-efficient sensitive elements for control systems in small satellites have been considered. Of practical interest is the creation of a ferromagnetic gyroscope. As its model, a periodic structure (a pseudocrystal) of coherent monodomain ferromagnetic quantum dots (FQDs) localized in spherical nanocontainers, where they are expected to dwell in the quantum levitation state, is proposed. Owing to the Einstein–de Haas effect, those FQDs would retain their angular momentum over time. To control the pseudocrystal orientation in space, the pseudocrystal is mounted on a movable platform located in an external two-component magnetic field (MF). The static component of the MF is perpendicular to the pseudocrystal base, and the dynamic component is perpendicular to the pseudocrystal lateral side. By analyzing the absorption spectrum of the dynamic MF and its dependence on the pseudocrystal orientation in space, it is possible to calculate the angular coordinates of the new pseudocrystal position, which are determined by the relative orientations of the fixed direction of the FQD's angular momentum and the vector of the external static MF.

K e y w o r d s: nanophysics, nanoparticle, ferromagnetic quantum dot, levitation, gyroscope, spin, magneton, angular momentum.

1. Introduction

Nanosatellites, i.e., ultra-small artificial satellites of the CubeSat (cube satellite) standard, have recently attracted increased interest. These are "cubes" $10 \times 10 \times 10$ cm^3 in size and up to 1 kg in mass. Their outer surfaces are equipped with solar batteries, whereas the inside contains microelectronic power elements, systems for receiving and transmitting signals, video cameras for making satellite images of the Earth's surface, and so forth. The disadvantages of CubeSat satellites consist in that they are small and possess limited energy capabilities. Their advantage is a wider scope of research areas and technologies that can be quickly implemented with relatively small financial costs.

In this connection, it is practically significant to consider the possibilities of nanophysics and nanotechnology in developing nanosized and energy-efficient sensitive elements for control systems in small satellites. In this way, the main interest is the creation of a ferromagnetic gyroscope with nanosized sensitive elements.

2. Model of a Nanosized Sensor for a Ferromagnetic Gyroscope

As a model of a ferromagnetic gyroscope, let us choose N spherically symmetric nanocontainers. Near the center of each of them, there is a ferromagnetic quantum dot (FQD) in the quantum levitation state (see Appendix). In other words, spherically symmetric objects with a characteristic size $d \leqslant 10$ nm (see below) are created from a ferromagnetic material. Those elementary structures compose a layered periodic structure with cubic symmetry (a ferromagnetic pseudocrystal with cubic symmetry). In such a structure, the FQDs are arranged equidistantly, with the distance a being equal to the diame-
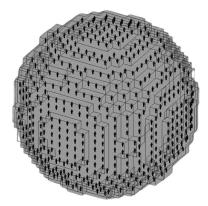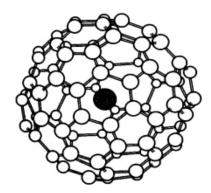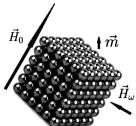
Fig. 1. Model of a ferromagnetic quantum dot

Fig. 2. A ferromagnetic quantum dot encapsulated into a nanocontainer

Fig. 3. Schematic vector diagram of a ferromagnetic gyroscope

ter of the spherically symmetric container, where the FQD is located, $a = 2r_0$ (see Figs 1 to 3).

After the technological implementation of the pseudocrystal, we obtain a matrix for the FQDs separated from one another by a distance sufficient to assume that only the magnetic dipole-dipole interaction takes place between the FQDs. Under such conditions, the issue of the influence of the pseudocrystal symmetry on the pseudocrystal's magnetic properties is eliminated, i.e., the cubic symmetry of the pseudocrystal is adopted only to specify the model.

In this work, we focus attention on the analysis of the physical principles for the functioning of a ferromagnetic gyroscope with nanosized sensitive elements (see Fig. 1) that compose a three-dimensional periodic, layered structure (see Fig. 3) of a given volume V (an artificial layered crystal consisting of nanosized sensitive elements). In other words, the obtained results of this research will have a qualitatively schematic character.

As a starting point for such an analysis, we chose the Einstein–de Haas effect [1–3] known from the course of general physics. Its essence is that, during the magnetization along a certain axis, a ferromagnet acquires an angular momentum (an angular impulse) $\mathbf{L} = $ const with respect to this axis, and the angular momentum $\mathbf{L}$ is proportional to the magnetic moment $\mathbf{M}$ of the ferromagnetic specimen.

Note that the authors of works [4,5] proposed to use the classical Einstein–de Haas [1–3] and Barnett [6–8] effects (the Barnett effect is, in a certain sense, opposite to the Einstein–de Haas one) for constructing ferromagnetic gyroscopes. However, in the case of massive crystals, these effects, taking the smallness of their quantitative parameters, were of purely academic interest. At the same time, in the case of nano-objects with quantum properties, the situation can be qualitatively different.

As was shown by theoretical and experimental studies [9–14], the magnetic moment of atoms in ferromagnetic crystals, as a result of the spin-orbit interaction and magnetic anisotropy, is substantially lower than the sum of uncompensated Bohr magnetons (the spin magnetic moments of electrons) of the same atoms. At the same time, a nanosized ferromagnet with a characteristic size of $1 \leqslant d \leqslant 12$ nm (and containing from 10 to 10^4 atoms), due to a reconstructing of the interaction and the dominant role of surface atoms over bulk ones, becomes monodomain, and its own magnetic moment approaches by magnitude to the vector sum of uncompensated Bohr magnetons of its atoms, thus becoming considerably larger [11, 12] in comparison with that in the case of ferromagnetic crystal.

Ensembles of nanosized ferromagnetic formations, which are characterized by extremely high specific magnetization (significantly exceeding the specific magnetization of the ferromagnetic crystal) in weak external magnetic fields, as well as by the absence of hysteresis, are called superparamagnets [11,13]. They

can be considered as "big blocks" for creating new materials and devices.

To achieve the goal of the work, it is necessary

• to consider the structure of nanosized sensitive elements and analyze their physical properties;

• to analyze the quantum states of nanosized sensitive elements, which are induced by the Einstein–de Haas effect;

• to consider the issue of quantum levitation of nanosized sensitive elements in a spherical nanosized container;

• to analyze the mechanism of monitoring a variation of the pseudocrystal orientation with respect to a fixed direction of the magnetic moment of nanosized sensitive elements owing to the conservation of their angular momentum.

Nowadays, the ferromagnetic formations of a required nanosize are mainly constructed from ions of transition elements. A lot of magnetic molecules are known [11, 12]: V_{15}, Fe_8, Fe_{10}, Fe_{30}, Mn_2Ac, Mn_6, Mn_{12}, an d o thers. Note that the manufacturing technology of nanosized ferromagnetic formations is now well-developed because of their wide application in medical and biological practice.

Let us also pay attention to the fact that nanoscale formations composed of ions of transition elements possess not only a magnetic moment, but also an uncompensated electric charge.

As a model of a sensitive element for a ferromagnetic gyroscope, let us consider a nanosized ferromagnetic sphere whose radius R is of an order of $1\ \text{nm} \leqslant R \leqslant 12\ \text{nm}$. Such a formation – it contains a small ($10 \div 10^4$) number of atoms; see Fig. 1 – is called differently: a nanoparticle, a nanocrystal, an artificial atom, or a quantum dot, because it still has quantum properties. In what follows, the term "ferromagnetic quantum dot" (FQD) will be used.

We assume that an FQD is encapsulated in a spherical nanocontainer (see Fig. 2), the radius of which is several dozen times larger than the FQD radius. The FQD is in the quantum levitation state as a material point that is located in a spherically symmetric potential well [20]; see Appendix. The levitation of FQD is necessary to exclude the influence of the environment on the FQD dynamics (as concerning friction, it is completely absent in this case).

FQDs are interesting, because they possess an additional internal degree of freedom, the monodomain magnetic moment **m**, which is responsible for a wide

variety of their properties and makes it possible to monitor and control their state with the help of an external magnetic field with the intensity $\mathbf{H}_0$.

As a sensitive element of a ferromagnetic gyroscope, we propose to consider an FQD that, being in the quantum levitation state, precesses in the external magnetic field, and whose magnetic moment **m** is formed to a large extent by its uncompensated spin subsystem.

A ferromagnetic gyroscope will be practically implementable provided that the quantum angular momentum $\mathbf{S}$ ($S = |\mathbf{S}| = N\frac{\hbar}{2}$) of the FQD, which is determined by the FQD's spin subsystem consisting of N uncompensated spins, substantially exceeds the classical FQD's mechanical angular momentum $\mathbf{l}_0 = \hat{J}_0\boldsymbol{\omega}_0$. Here, $J_0 = \frac{2}{5}m_0R^2$ is the classical moment of inertia of a ferromagnetic sphere with the inert mass m_0 and the radius R, which rotates at the cyclic frequency of the classical Einstein–de Haas effect ω_0. Only provided this condition is satisfied, from whence, the following inequality holds:

$$\omega \simeq \frac{S}{J_0} \gg \omega_0, \tag{1}$$

the magnetized FQD is in a state of rotational motion at the frequency ω; i.e., there arises the Einstein–de Haas supereffect.

As a result, the mechanical angular momentum **j** of the FQD, which is preserved, can be determined by the formula

$$\mathbf{j} = \mathbf{l}_0 + \mathbf{S}, \tag{2}$$

where $\mathbf{S} = \text{const}$ and $\mathbf{l_0} \ll \mathbf{S}$. Accordingly, we may assume that the angular momentum vector of the pseudocrystal, $\mathbf{J} = \text{const}$, is determined by the vector sum

$$\mathbf{J} = \sum_{i=1}^{N} \mathbf{j}_i \simeq \sum_{i=1}^{N} \mathbf{S}_i \tag{3}$$

of uncompensated FQD spins, which was previously known from experimental studies [11–14].

The magnitude of the FQD's magnetic moment is determined by the chain of formulas

$$m = \mu_{\mathrm{B}}N = \mu_{\mathrm{B}}\frac{2S}{\hbar} = -\gamma S, \tag{4}$$

where $\mu_{\mathrm{B}} = \frac{e\hbar}{2m_ec}$ is the Bohr magneton (the elementary magnetic moment of electron), and $\gamma = \frac{|e|}{m_ec}$ is the electron gyromagnetic ratio. According to formu-

la (1), the FQD rotation frequency equals

$$\omega \simeq \frac{S}{J_0} = \frac{5}{4}\frac{N\hbar}{m_0 R^2}, \quad N \gg 1, \quad \omega \gg \omega_0. \tag{5}$$

Let us evaluate the quantity ω. It is obvious that the quantities N and R are interdependent. Let us find a functional relationship between them. For this purpose, the FQD and its structural element will be considered as spheres with the radii R and r_a, respectively. The relationships between their volumes V and V_a, respectively, and their inert masses m_0 and m_a, respectively, will be written as follows: $V \simeq$ $\simeq NV_a/k$ and $m_0 \simeq Nm_a/k$, where k is the number of uncompensated spins in the FQD structural element. Then the number N of uncompensated FQD spins in the volume V and the quantity ω have the following representations:

$$N = k\left(\frac{R}{r_a}\right)^3, \quad \omega = \frac{5}{4}\frac{k\hbar}{m_a R^2}. \tag{6}$$

Let us make a quantitative evaluation of N and ω using the example of such an FQD structural element as an iron atom, for which $m_a = 9.27 \times 10^{-23}$ g, $r_a = 1.2 \times 10^{-8}$ cm, and $k = 4$. In this case, for a FQD with the characteristic size $R \simeq 1$ nm, we obtain

$$N \simeq 4 \times 72 = 289, \quad \omega \simeq 1.43 \times 10^{11} \text{ s}^{-1}. \tag{7}$$

It is essential that an FQD with $R \simeq 1$ nm, which remains in the quantum levitation state, rotates at an angular velocity of an order of 10^{11} s^{-1} (inertial motion) only because it has the monodomain magnetic moment $\mathbf{m}$, without any energy costs (the Einstein–de Haas supereffect).

To evaluate the magnitude $B_{\mu_{\rm B}}$ of the magnetic field induction of the FQD associated with its magnetic moment m, let us use the equality $B_{\mu_{\rm B}} m \simeq \hbar\omega$. Whence, in view of formulas (1) and (4), we obtain

$$B_{\mu_{\rm B}} \simeq \frac{\hbar\omega}{\gamma S} = \frac{\hbar}{\gamma J_0}. \tag{8}$$

By order of magnitude, the induction of the magnetic field of FQD, formula (8), has the following value:

$$B_{\mu_{\rm B}} \simeq 5 \times 10^3 \text{ Gs}. \tag{9}$$

Formula (9) testifies that the magnetic moment $\mathbf{m}$ of FQD creates a substantial magnetodipole field, which has to be taken into account in the further calculations.

Thus, we have found a physical justification for the prospective application of FQDs as sensitive elements in ferromagnetic gyroscopes.

The work [15] and the references therein are useful for understanding the physics of artificial magnetic materials. In those works, magnetic composites were considered which can be created by embedding super-paramagnetic nanoparticles into a liquid, polymer, or solid simple cubic matrix.

When designing a device based on a really operating pseudocrystal model, the fact has to be taken into account that the FQD is a quasi-classical object, which should be isolated from external influences by engaging that or another levitation mechanism. In the specialized scientific literature, one can find theoretical descriptions of various mechanisms of levitation of macroscopic objects. The most famous mechanism of levitation of macroscopic ferromagnetic objects is the Meissner effect [16–19]. It is the Meissner effect that explains the levitation of a superconductor over a strong magnet (or a magnet over a superconductor). However, the implementation of levitation of an ordered ensemble of FQDs on the basis of the Meissner effect is not very promising due to its technological complexity.

Bearing the purpose of this work in mind, as well as from our viewpoint, more promising is the quantum levitation of the FQD in a suitable nanocontainer, with the latter playing the role of a deep potential well for the FQD [20]. Such a model has not been previously considered in the scientific literature. In this case, the problem of FQD isolation from the influence of the environment is solved automatically due to the mechanism of quantum levitation of FQD in the nanocontainer (see Appendix and Fig. 2).

From the application viewpoint, it is reasonable to rigidly fix the lower face of the pseudocrystal at the moving platform located in an external uniform magnetostatic field with the strength $\mathbf{H}_0$. It is appropriate to direct the magnetostatic field $\mathbf{H}_0$ perpendicularly to the moving platform, where this pseudocrystal is mounted.

Taking the law of conservation J of the total FQD angular momentum into account, $\mathbf{J} = \text{const}$, a variation in the spatial orientation of the moving platform will change the direction of the vector of the total magnetic field induction $\mathbf{B}_{\rm res}$, which is a vector sum of the magnetostatic field $\mathbf{H}_0$ and the magnetodipole field $\mathbf{B}$ of pseudocrystal induced by the magnetic mo-

ments $\mathbf{m}$ of FQDs (see below). In turn, monitoring the induction of the magnetic field $\mathbf{B}_{\mathrm{res}}$ will make it possible to obtain data on the orientational dynamics of the flying object.

In order to control the orientational dynamics of the object flying over the geometric center of the upper face of the pseudocrystal, it is necessary to mount a magnetometer sensor. The latter is used to measure the induction of the resulting magnetic field $\mathbf{B}_{\mathrm{res}} = \mathbf{H}_0 + \mathbf{B}$. As will be shown below, the components of the induction vector of the resulting magnetic field $\mathbf{B}_{\mathrm{res}}$ contain information on the spatial orientation change of the pseudocrystal, i.e., the data on the orientational dynamics of the flying object.

3. Analysis of Pseudocrystal Magnetization Dynamics

Let us introduce a Cartesian coordinate system $OXYZ$, with the origin point O located at the geometric center of the pseudocrystal and the axes X, Y, and Z being parallel to the pseudocrystal edges. Denote the unit vectors of this coordinate system as $\mathbf{e}_x, \mathbf{e}_y$, and $\mathbf{e}_x$. Let there be $2N_{1,2,3} + 1$ FQDs along the axes X, Y, and Z. Hereafter, $N_{1,2,3}$ are integer numbers. So, the total number of FQDs in the pseudocrystal equals $N = (2N_1 + 1)(2N_2 + 1)(2N_3 + 1)$. The coordinates of each FQD are determined by the radius vector $\mathbf{r_n} = a\mathbf{n}$, where $\mathbf{n} = (n_1, n_2, n_3)$ and $n_{1,2,3} = 0, \pm 1, \pm 2, ..., \pm N_{1,2,3}$. Taking the properties of FQDs [11, 12] and their remoteness from one another, it is admissible to assume that there exists only magnetodipole interaction between them.

In the selected coordinate system, the induction of the magnetodipole field $\mathbf{B_n} = \mathbf{B_n}(\mathbf{r})$ created by an FQD with the coordinates $r_\mathbf{n}$ can be written in the form

$$\mathbf{B_n} = -\left[\frac{\mathbf{m}}{|\mathbf{r} - \mathbf{r_n}|^3} - 3\frac{\hat{D}(\mathbf{r} - \mathbf{r_n})\mathbf{m}}{|\mathbf{r} - \mathbf{r_n}|^5}\right]. \tag{10}$$

According to the superposition principle, the magnetodipole field $\mathbf{B}_d$ of the pseudocrystal can be written

as follows:

$$\mathbf{B}_d = -\sum_\mathbf{n}\left[\frac{\mathbf{m}}{|\mathbf{r} - \mathbf{r_n}|^3} - 3\frac{\hat{D}(\mathbf{r} - \mathbf{r_n})\mathbf{m}}{|\mathbf{r} - \mathbf{r_n}|^5}\right]. \tag{11}$$

For further calculations, it is pertinent to express vector (11) via the pseudocrystal magnetization

$$\mathbf{M} = \frac{1}{V}\sum_\mathbf{n}\mathbf{m} \quad \text{or} \quad \mathbf{M} = \frac{\mathbf{m}}{a^3} \tag{12}$$

in the following form:

$$\mathbf{B}_d = -\hat{G}(\mathbf{r})\mathbf{M}, \tag{13}$$

where

$$\hat{G} = a^3\sum_\mathbf{n}\left[\frac{1}{|\mathbf{r} - \mathbf{n}|^3} - 3\frac{\hat{D}(\mathbf{r} - \mathbf{n})}{|\mathbf{r} - \mathbf{n}|^5}\right]$$

is the geometric factor (the discrete demagnetizing factor) of the pseudocrystal, and $V = a^3 N$ is the pseudocrystal volume.

According to the superposition principle, the induction of the magnetic field created by the pseudocrystal in the magnetostatic field $\mathbf{H}_0$ is determined by the formula

$$\mathbf{B}_{\mathrm{res}} = \mathbf{H}_0 + \mathbf{B}_d. \tag{14}$$

Since the magnetic moment of each FQD is proportional to its conserved angular momentum, the magnetic moments of the FQDs will also retain their directions in space, if the pseudocrystal orientation changes. This means that due to the preservation of the FQD angular momenta, the spatial orientation of the vector $\mathbf{B}_d$ will be unchanged. At the same time, if the pseudocrystal orientation changes, the vector $\mathbf{B}_{\mathrm{res}} = \mathbf{H}_0 + \mathbf{B}_d$ will also vary, which makes it possible to trace the orientation change of the flying object.

If the pseudocrystal orientation changes, the transition to a new coordinate system $OX'Y'Z'$ associated with the pseudocrystal is described by the matrix

$$\hat{R} = \begin{pmatrix} c(\gamma) + e_x{}^2 w(\gamma) & e_x e_y w(\gamma) - e_z s(\gamma) & e_x e_z w(\gamma) + e_y s(\gamma) \\ e_y e_x w(\gamma) + e_z s(\gamma) & c(\gamma) + e_y{}^2 w(\gamma) & e_y e_z w(\gamma) - e_x s(\gamma) \\ e_z e_x w(\gamma) - e_y s(\gamma) & e_z e_y w(\gamma) + e_x s(\gamma) & c(\gamma) + e_z{}^2 w(\gamma) \end{pmatrix}, \tag{15}$$

where $s(\gamma) = \sin(\gamma)$, $c(\gamma) = \cos(\gamma)$, $w(\gamma) = 1 - \cos(\gamma)$, the unit vector $\mathbf{e} = \mathbf{e}_{z'}$ defines the direction of the Z'-axis in the coordinate system $OX'Y'Z'$, and γ is the rotation angle of the coordinate system $OX'Y'Z'$ around the vector $\mathbf{e}$. Note that the components of the vector

$$\mathbf{e} = (\sin(\alpha)\cos(\beta), \sin(\alpha)\sin(\beta), \cos(\alpha))$$

are determined in the coordinate system $OXYZ$, where α and β are the polar and azimuthal angles, respectively.

The components of the FQD magnetic moment $\mathbf{m}$ in the coordinate system $OX'Y'Z'$ are determined by the rotation matrix $\mathbf{m}' = \hat{R}(\mathbf{e}, \gamma)\mathbf{m}$, and the magnetodipole field vector obviously has the following form near the point $\mathbf{r}$:

$$\mathbf{B}'_d = \sum_{\mathbf{n}} \hat{R}(\mathbf{e}, \gamma)\hat{G}(\mathbf{r})\mathbf{M}. \tag{16}$$

In particular, formula (16) can be applied in gyroscopy as follows.

1. Magnetostatic approach. In the general case, the induction of the resulting magnetic field $\mathbf{B}'_{\text{res}}$ in a vicinity of the magnetometer sensor is determined by the formula

$$\mathbf{B}'_{\text{res}} = \mathbf{H}'_0 + \mathbf{B}'_d(\mathbf{r}'_{N_3}). \tag{17}$$

In this formulation of the problem, the magnetization of the pseudocrystal is almost uniform. Therefore, the subscript N_3 in formula (17) will be omitted below.

Formula (17) has an application potential for gyroscopy, since the main task of the latter is to monitor the orientation changes of a flying object. In particular, if the vector $\mathbf{B}_{\text{res}}$ is determined using a magnetometer in the case $\mathbf{H}_0 = 0$, then formula (17) can be considered as a system of three equations for the unknown angles α, β, and γ, which describe the new orientation of pseudocrystal. In other words, the system of equations (17) describing the induction of the magnetic field created by a ferromagnetic pseudocrystal can be considered as a physical basis for the development of a ferromagnetic gyroscope.

2. Magnetodynamic approach. The magnetodynamic approach looks more promising from the application viewpoint. In particular, if $\mathbf{H}_0 \neq 0$, the magnetic moments $\mathbf{m}$ of FQDs in the pseudocrystal are in the precession state. Provided that a uniform harmonic magnetic field (HMF) $\mathbf{H}_\omega$ with the cyclic frequency ω_z is created between two side faces of the pseudocrystal and perpendicularly to the magnetostatic field $\mathbf{H}_0$, then intensive absorption of its energy will occur in a vicinity of the Larmor frequencies of the magnetic moments $\mathbf{m}$ of FQDs. This phenomenon can be used to determine the spatial orientation change of the pseudocrystal.

Under the condition $N_{1,2,3} \gg 1$, the FQDs in the pseudocrystal bulk can be assumed to play the main role in the energy absorption of the HMF $\mathbf{H}_\omega$. Therefore, we may consider the total induction of the magnetic field

$$\mathbf{B}'_f = \mathbf{B}_d + \mathbf{H}_0 + \mathbf{H}_\omega \tag{18}$$

to be uniform within the pseudocrystal and close by magnitude to that at the center of pseudocrystal. If the dimensions of pseudocrystal are chosen such that $1 \ll N_3 \ll N_{1,2}$, then, according to works [21, 22], the geometric factor (the discrete demagnetizing factor) and the magnetodipole field have only one non-zero component each:

$$G_{z'z'} = 4\pi, \quad \mathbf{B}'_d = (0, 0, -4\pi M_{z'}). \tag{19}$$

In this approximation, the nonlinear Landau–Lifshitz dynamic equation (12) for the pseudocrystal magnetization in the coordinate system $OX'Y'Z'$ looks like

$$\frac{d\mathbf{M}'}{dt} = -\gamma[\mathbf{B}'_f \times \mathbf{M}'] - \frac{\beta}{M_0{}^2}[[\mathbf{B}'_f \times \mathbf{M}'] \times \mathbf{M}'], \tag{20}$$

where γ is the gyromagnetic ratio, $0 < \beta \ll 1$ is the damping coefficient, and $M_0 = |\mathbf{M}'|$. By scalar multiplying Eq. (20) by the vector $\mathbf{M}'$ and considering the properties of the mixed vector product on the right-hand side of Eq. (20), we come to the conclusion that $|\mathbf{M}'| = \text{const}$. This result means that the dynamics of the vector $\mathbf{M}'$ in the magnetic field with the induction $\mathbf{B}'_f$ is reduced to precession.

Let us specify the intensity of the external magnetic field $\mathbf{H}'_f$ as follows:

$$\begin{cases} \mathbf{H}'_f = (H_{\omega x'}, H_{\omega y'}, H_{0z'} + H_{\omega z'}), \\ \mathbf{H}'_\omega = \mathbf{H}'_1 e^{i\omega_{z'}t} \end{cases} \tag{21}$$

where $\omega_{z'}$ is the cyclic frequency of the harmonic magnetic field. In this case, the magnetic field induction in Eq. (20) has the following representation:

$$\mathbf{B}'_f = \mathbf{B}'_d + \mathbf{H}'_f. \tag{22}$$

From the mathematical viewpoint, Eq. (20) is similar to those that were analyzed in the magnetic resonance theory [21, 22], usually at small deviation angles between the vectors $\mathbf{M}'$ and $\mathbf{B}'_f$. In our case, such a restriction is not acceptable.

To construct the general solution of Eq. (20), let us select the ansatz

$$
\begin{cases}
M'_{0x'} = M_0 \sin(\theta) \cos(\varphi), \\
M'_{0y'} = M_0 \sin(\theta) \sin(\varphi), \\
M'_{0z'} = M_0 \cos(\theta)
\end{cases}
\tag{23}
$$

as a trial function. Here, where $M_0 = |\mathbf{M}'|$; and $\theta = \theta(t)$ and $\varphi = \varphi(t)$ are the polar and azimuthal, respectively, angles, which are the dynamic variables of the problem under the condition $|\mathbf{M}'| = M_0 = \text{const}$.

We have the following relationships between the components of the vector $\mathbf{M}'$ and the dynamic angular variables θ and φ:

$$
\theta = \arccos\left(\frac{M'_{0z'}}{M_0}\right), \quad \varphi = \arctan\left(\frac{M'_{0y'}}{M'_{0x'}}\right).
\tag{24}
$$

For further calculations, it is convenient to express the magnetic field induction $\mathbf{B}'_f$ via the potential energy U of magnetization $\mathbf{M}'$ in this field. It can be done as follows:

$$
B'_{fi} = -\frac{\partial U}{\partial M'_i} = -\frac{\partial U}{\partial \theta}\frac{\partial \theta}{\partial M'_i} - \frac{\partial U}{\partial \varphi}\frac{\partial \varphi}{\partial M'_i},
\tag{25}
$$

where $i = x', y', z'$. The relationships between the components of the magnetic field in the Cartesian and spherical coordinate systems were found in the following form:

$$
\begin{aligned}
B_{fx'} &= -\frac{\partial U}{\partial M_{fx'}} = -\sin(\varphi) B_{f\varphi}, \\
B_{fy'} &= -\frac{\partial U}{\partial M_{fy'}} = +\cos(\varphi) B_{f\varphi}, \\
B_{fz'} &= -\frac{\partial U}{\partial M_{fz'}} = -\frac{1}{\sin(\theta)} B_{f\theta},
\end{aligned}
\tag{26}
$$

where

$$
\begin{cases}
B_{f\theta} = -\dfrac{1}{M_0}\dfrac{\partial U}{\partial \theta}, \\
B_{f\varphi} = -\dfrac{1}{M_0 \sin(\theta)}\dfrac{\partial U}{\partial \varphi}
\end{cases}
\tag{27}
$$

are the components of the magnetic field $\mathbf{B}'_f$ in the spherical coordinate system, which were found from formulas (24).

Substituting Eqs. (26) into Eq. (20) and performing some algebraic simplifications, we obtain

$$
\begin{cases}
\dfrac{\partial \theta}{\partial t} + \gamma B_{f\varphi} = \dfrac{\beta}{M_0} B_{f\theta}, \\
\dfrac{\partial \varphi}{\partial t} - \dfrac{\gamma}{\sin(\theta)} B_{f\theta} = \dfrac{\beta}{M_0 \sin(\theta)} B_{f\varphi}.
\end{cases}
\tag{28}
$$

The system of equations (28) is equivalent to the Landau–Lifshitz equation (20) and has a wide scope of applications. It can be used for an arbitrary amplitude of oscillations of the vector $\mathbf{M}'$ and at any level of nonlinearity.

In what follows, we assume that the HMF $\mathbf{B}_\omega$ is a small perturbation to the magnetostatic field $\mathbf{H}_0$ and use the criterion $|\mathbf{H}_1| \ll |\mathbf{H}_0|$ in order to linearize the system of equations (28) in a vicinity of the steady state of the system. For this purpose, we write down the potential energy of magnetization in the form

$$
U = U_0 + U_1,
\tag{29}
$$

where is the first summand,

$$
U_0 = -H_0 M_0 \cos(\theta) + 2\pi M_0{}^2 \cos^2(\theta),
\tag{30}
$$

determines the potential energy of magnetization $\mathbf{M}'$ in the magnetostatic field, and the second one,

$$
\begin{aligned}
U_1 &= -H_\omega M_0 \big(\sin(\theta)\sin(\theta_1)\cos(\varphi - \varphi_1) + \\
&\quad + \cos(\theta)\cos(\theta_1) \big), \\
H_\omega &= H_1 \exp(i\omega_{z'}t),
\end{aligned}
\tag{31}
$$

where

$$
H_\omega = H_1 \exp(i\omega_{z'}t),
$$

does the same in the HMF $\mathbf{H}'_\omega$. In Eqs. (30) and (31), $\theta_1 = \text{const}$ and $\varphi_1 = \text{const}$ are the angular coordinates of the vector $\mathbf{H}_1$. It is quite clear that only the real parts of the quantity U_1 and the formulas obtained on its basis have a physical meaning.

By substituting Eqs. (29)–(31) into Eqs. (27), we obtain the magnetic field (27) in the following form:

$$
\begin{cases}
B_{f\theta} = -H_0\Big(1 - 4\pi \dfrac{M_0}{H_0}\cos(\theta)\Big)\sin(\theta) + \\
\quad + H_\omega \big(\cos(\theta)\sin(\theta_1)\cos(\varphi - \varphi_1) - \\
\quad - \sin(\theta)\cos(\theta_1) \big), \\
B_{f\varphi} = -H_\omega \sin(\theta)\sin(\theta_1)\sin(\varphi - \varphi_1), \\
H_\omega = |\mathbf{H}'_1| e^{i\omega_{z'}t}.
\end{cases}
\tag{32}
$$

A combination of formulas (28) and (32) brings the dynamic equations of the problem to the form

$$
\begin{cases}
\dfrac{\partial \theta}{\partial t} = - \left[\alpha \omega_\theta - (a_\varphi + \alpha a_\theta)\omega_1 e^{i\omega_{z'}t} \right] \sin(\theta), \\[2mm]
\dfrac{\partial \varphi}{\partial t} = -\omega_\theta + (a_\theta - \alpha a_\varphi)\omega_1 e^{i\omega_{z'}t},
\end{cases}
\tag{33}
$$

where

$$
\begin{aligned}
&\omega_\theta = \omega_0 \left[1 - \lambda \cos(\theta) \right], \ \omega_0 = \gamma H_0, \ \lambda = 4\pi \frac{M_0}{H_0}, \\
&a_\theta = \cot(\theta)\sin(\theta_1)\cos(\varphi - \varphi_1) - \cos(\theta_1), \\
&a_\varphi = \sin(\theta_1)\sin(\varphi - \varphi_1), \\
&\alpha = \frac{\beta}{\gamma M_0} \quad \omega_1 = \gamma H_1.
\end{aligned}
\tag{34}
$$

Equations (33) are exact. Let us first consider the stationary dynamics of the magnetization vector $\mathbf{M}'$ in the magnetostatic field $\mathbf{H}'_0$ and its dependence on various factors

In the simplest case, i.e., without considering the demagnetizing field and dissipation processes, $\beta = 0$, solutions of Eqs. (28) look like

$$
\begin{cases}
\theta = \theta_0 = \text{const}, \\
\varphi = \varphi_0 = \phi_0 - \omega_0 t, \quad \phi_0 = \text{const}.
\end{cases}
\tag{35}
$$

Hence, in this case, the dynamics of the vector $\mathbf{M}'$ is reduced to the precession around the vector $\mathbf{H}'_0$ with the cyclic frequency $\omega_0 = \gamma \mathbf{H}'_0$, as it has to be.

If we account for the demagnetizing field at $\beta = 0$, then the solutions of Eqs. (28), namely,

$$
\begin{cases}
\theta = \theta_0 = \text{const}, \\
\varphi = \varphi_0 = \phi_0 - \omega_{\theta_0} t, \quad \phi_0 = \text{const}, \\
\omega_{\theta_0} = \omega_0 \left[1 - \lambda \cos(\theta_0) \right],
\end{cases}
\tag{36}
$$

acquire a new quality: the precession frequency $\omega_0 \rightarrow \omega_{\theta_0}$ becomes dependent on the angle θ_0 between the directions of the vectors $\mathbf{H}'_0$ and $\mathbf{M}'_0$.

Dissipation processes, $\beta \neq 0$, substantially complicate the solutions of the system of equations (28). For instance, without the influence of a demagnetizing field and at $\beta \neq 0$, they include an implicit function of the dynamic variable θ,

$$
\begin{cases}
\tan\left(\dfrac{\theta}{2}\right) = \tan\left(\dfrac{\theta_0}{2}\right) e^{-\alpha \omega_0 t}, \quad \theta_0 = \text{const}, \\[2mm]
\varphi = \varphi_0 = \phi_0 - \omega_0 t, \quad \phi_0 = \text{const}.
\end{cases}
\tag{37}
$$

Formulas (37) describe the damping precession with the frequency ω_0 and the damping parameter $\alpha \omega_0$.

In the most general case, the magnetostatic dynamics of the magnetization $\mathbf{M}'$ is described by the solutions of the system of equations (28)

$$
\begin{cases}
A(\theta) = A(\theta_0)e^{-\alpha \omega_0 t}, \\[2mm]
\varphi = \varphi_0 = \phi_0 - \omega_0 \left[t - \lambda \displaystyle\int_0^t \cos\theta(\tau)d\tau \right],
\end{cases}
\tag{38}
$$

where

$$
A = \frac{\tan\left(\frac{\theta}{2}\right)^{\frac{1}{1-\lambda}}}{\left[\tan\left(\frac{\theta}{2}\right)^2 + \frac{1-\lambda}{1+\lambda} \right]^{\frac{\lambda}{1-\lambda^2}}},
\tag{39}
$$

which were obtained at $\mathbf{H}'_\omega = 0$ and are expressed via an implicit function of the dynamic variable θ. It is obvious that, at $\lambda = 0$, formulas (38) are reduced to formulas (37).

The obtained solutions (38) of the system of equations (28) with $\mathbf{H}'_\omega = 0$ are exact. From formulas (38), it follows that the demagnetizing field and dissipation processes substantially affect the precession character of the vector $\mathbf{M}'$. In particular, the cyclic precession frequency

$$
\omega_{\theta_0} = \omega_0 \left[1 - \lambda \cos(\theta) \right]
\tag{40}
$$

depends on the angle θ between the vectors $\mathbf{M}'$ and $\mathbf{H}'_0$. Furthermore, due to dissipation processes ($0 < \beta \ll 1$), the angle θ slowly changes in time within the interval $0 < \theta < \theta_0$.

Now, let us consider the influence of the HMF $\mathbf{H}'_\omega$ (see Fig. 3) on the dynamics of the pseudocrystal magnetization vector $\mathbf{M}'$. Since this problem is essentially nonlinear, it is impossible to find an exact solution to the system of equations (28). Therefore, we limit the consideration to solving them in the linear approximation.

As a rule, when linearizing the Landau–Lifshitz equation in the ferromagnetic resonance theory, the Smit–Suhl method [23–26] is applied. When using this method as a reference solution for the dynamic equations of the problem, the magnetization equilibrium condition is applied, when the effective magnetic field (27) equals zero. However, in this work, owing to the Einstein–de Haas effect [1–3], such a magnetization state is impossible. Magnetization in this case

will always be in the precession. Therefore, when linearizing the system of equations (28), it is necessary to choose their stationary solution (36) or (38) as a reference one.

Taking the character of the system perturbations by the HMF $\mathbf{H}'_\omega$, let us choose the dynamic variables of the problem in the following form:

$$\theta = \theta_0 + \delta\theta, \ \varphi = \varphi_0 + \delta\varphi, \quad \delta\theta \ll 1, \ \delta\varphi \ll 1, \quad (41)$$

where the quantities $\theta_0 = \text{const}$ and $\varphi_0 = \phi_0 - \omega_{\theta_0}t$ correspond to the stationary state of the system, which is determined by solutions (36) of the system of equations (28) where the dissipation processes are neglected ($\beta = 0$). Later, we will take them into account using the standard frequency reduction $\omega_{\theta_0} \rightarrow \omega_{\theta_0} + i\alpha\omega_{z'}$ [21, 22]

and representation (41) for the dynamic variables of the problem in Eqs. (32) and (28), we obtain the following system of inhomogeneous linear equations for the quantities $\delta\theta$ and $\delta\varphi$:

$$\begin{cases} \dfrac{d\delta\theta}{dt} = \omega_1 \sin(\theta_1) \sin(\chi_1) e^{i\omega_{z'}t}, \\[2mm] \dfrac{d\delta\varphi}{dt} = \omega_1\big(\text{ctg}(\theta_0) \sin(\theta_1) \cos(\chi_1) - \\[2mm] - \cos(\theta_1)\big)e^{i\omega_{z'}t}, \end{cases} \quad (42)$$

where $\omega_1 = \gamma H_1$, $\chi_1 = \varphi_0 - \varphi_1$, and $\varphi_0 = \phi_0 - \omega_{\theta_0}t$.

The solution of the system of equations (42) reads

$$\begin{cases} \delta\theta = \dfrac{\omega_1\omega_{cs}(\chi_1)}{\omega_{\theta_0}{}^2 - \omega_{z'}{}^2} \sin(\theta_1) e^{i\omega_{z'}t}, \\[3mm] \delta\varphi = -\Big(\dfrac{\omega_1\omega_{sn}(\chi_1)}{\omega_{\theta_0}{}^2 - \omega_{z'}{}^2} \text{ctg}(\theta_0) \sin(\theta_1) + \\[3mm] + \dfrac{\omega_1}{i\omega_{z'}} \cos(\theta_1)\Big)e^{i\omega_{z'}t}, \end{cases} \quad (43)$$

where the quantities

$$\begin{aligned} \omega_{cs} &= \omega_{\theta_0} \cos(\chi_1) + i\omega_{z'} \sin(\chi_1), \\ \omega_{sn} &= \omega_{\theta_0} \sin(\chi_1) - i\omega_{z'} \cos(\chi_1) \end{aligned} \quad (44)$$

have a clearly pronounced resonance near the frequency $\omega_{\theta_0} = \omega_0 [1 - \lambda \cos(\theta_0)]$, which depends on the parameter θ_0. In addition, the oscillation amplitudes of the quantities $\delta\theta$ and $\delta\varphi$ depend on the time, since the quantity χ_1 in Eqs. (44) is a periodic function of time; this fact substantially affects

the dynamics of the $\mathbf{M}'$ vector. Let us also pay attention to that, in the case of collinear vectors $\mathbf{H}'_1$ and $\mathbf{H}'_0$ ($\theta_1 = [0, \pi]$), the harmonic magnetic field $\mathbf{H}'_\omega$ does not appreciably affect the dynamics of the vector $\mathbf{M}'$. In this connection, we will consider the cases where $\theta_1 = 90°$.

For the numerical analysis of the problem, let us change to dimensionless variables, namely,

$$\begin{aligned} &\tau = \omega_0 t, \ \overline{\omega}_{\theta_0} = \dfrac{\omega_{\theta_0}}{\omega_0}, \ \overline{\omega}_{z'} = \dfrac{\omega_{z'}}{\omega_0}, \ \overline{\omega}_1 = \dfrac{\omega_1}{\omega_0}, \\ &\overline{\omega}_{cs} = \dfrac{\omega_{cs}}{\omega_0}, \ \overline{\omega}_{sn} = \dfrac{\omega_{sn}}{\omega_0}, \ \varphi_0 = \phi_0 - \overline{\omega}_{\theta_0}\tau. \end{aligned} \quad (45)$$

If substitutions (45) are made in formulas (43), the latter retain their form and present expressions for the quantities $\delta\theta$ and $\delta\varphi$ in terms of dimensionless variables (45).

First of all, let us consider the free precession of the relative magnetization vector $\mathbf{J} = \mathbf{M}/M_0$ on the basis of formulas (36) written in terms of dimensionless variables (45) for the values of the polar angle $\theta_0 = 30°$, $60°$, and $90°$, and the demagnetization parameter $\lambda = 0.25$. The plots of precessions under those conditions are shown in Fig. 4. Let us take the motion path of the vector $\mathbf{J}$ at $\theta_0 = 90°$ as the reference one. In particular, in this case, the demagnetizing field has no effect on the dynamics of the vector $\mathbf{J}$, the precession period equals $\tau_{90°} = 2\pi$, and the orbit radius is $r_{90°} = 2\pi$. Note that, here, the planes of the orbits of the $\mathbf{J}$ vector are parallel to the plane $O'X'Y'$.

Concerning the precession period of the vector $\mathbf{J}$ provided other conditions are satisfied, it is determined by the formula $\tau_{\theta_0} = \frac{2\pi}{1 - \lambda\cos(\theta_0)}$. This formula explains why, in Fig. 4, the motion paths of the vectors $\mathbf{J}_{\theta_0}$ with the rotation period $\tau_{\theta_0} > \tau_{90°}$ are incomplete within the time interval $0 \geq \tau \geq \tau_{90°}$.

Now, let us consider the influence of the HMF frequency $\mathbf{H}'_\omega$ on the precession of the vector $\mathbf{M}'$. The corresponding plots of the motion paths of the vector $\mathbf{J}$ are shown in Fig. 5 for various values of the parameter $\Delta\overline{\omega}$, the deviation of the frequency $\overline{\omega}$ from the resonance frequency. Each motion path was calculated within the corresponding rotation period of the vector $\mathbf{J}$. As follows from the plots depicted in Fig. 5, the HMF $\mathbf{H}'_\omega$ substantially affects the dynamics of the $\mathbf{M}'$ vector only in a vicinity of the resonance frequency.
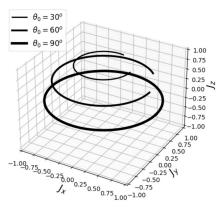
Fig. 4. Motion paths of the relative magnetization vector $\mathbf{J}$ for some values of the polar angle θ_0

Next, let us consider the dependence of the motion paths of the pseudocrystal magnetization vector $\mathbf{M}'$ on the magnitude of the HMF $\mathbf{H}_1'$ amplitude under resonance conditions. The corresponding plots for some values of the quantity $\omega_1 = \gamma|\mathbf{H}_1'|$ are shown in Fig. 6. As was done earlier, each motion path was calculated within the corresponding rotation period of the vector $\mathbf{J}$. One can see from the plots shown in Fig. 6 that the behavior of the motion paths of the vector $\mathbf{M}'$ substantially depends on the polar angle θ_0 and the amplitude of the HMF $\mathbf{H}_1'$, even if the quantity $\omega_1 = \gamma H_1$ changes slightly.

4. Absorption of the Energy of the Harmonic Magnetic Field by the Pseudocrystal

To analyze the intensity of absorption of the HMF $\mathbf{H}_\omega'$ energy, it is necessary to find the magnetic susceptibility tensor $\hat{\chi}$. The latter is determined by the variational derivatives,

$$\chi_{i'j'} = \frac{\delta M_{i'}}{\delta H_{\omega j'}'}, \quad i', j' = x', y', z'. \tag{46}$$

In order to specify formula (46), let us first rewrite expressions (43) for $\delta\theta$ and $\delta\varphi$ using the Cartesian components of the vector $\mathbf{H}_\omega'$. The result looks like

$$\begin{cases} \delta\theta = \gamma\dfrac{\omega_{cs}(\varphi_0)H_{1x'} + \omega_{sn}(\varphi_0)H_{1y'}}{\omega_{\theta_0}{}^2 - \omega_{z'}{}^2}e^{i\omega t}, \\ \delta\varphi = -\gamma\left(\dfrac{\omega_{sn}(\varphi_0)H_{1x'} - \omega_{cs}(\varphi_0)H_{1y'}}{\omega_{\theta_0}{}^2 - \omega_{z'}{}^2} \times \right. \\ \left. \times\,\mathrm{ctg}(\theta_0) + \dfrac{1}{i\omega_{z'}}H_{1z'}\right)e^{i\omega t}. \end{cases} \tag{47}$$

A combination of formulas (23), (41), (46), and (47) allows the magnetic susceptibility tensor $\hat{\chi}$ of the pseudocrystal to be found in the Cartesian coordinate system in the form

$$\hat{\chi} = \begin{pmatrix} \tau_{cs}\omega_{\theta_0} & -i\tau_{cs}\omega_{z'} & \chi_{sn} \\ i\tau_{cs}\omega_{z'} & \tau_{cs}\omega_{\theta_0} & -\chi_{cs} \\ -\tau_{sn}\omega_{cs} & -\tau_{sn}\omega_{sn} & 0 \end{pmatrix}, \tag{48}$$

$$\tau_{cs} = \frac{\gamma M_0\cos(\theta_0)}{\omega_{\theta_0}{}^2 - \omega_{z'}{}^2}, \quad \chi_{sn} = \frac{\gamma M_0\sin(\varphi_0)}{i\omega_{z'}}\sin(\theta_0),$$

$$\tau_{sn} = \frac{\gamma M_0\sin(\theta_0)}{\omega_{\theta_0}{}^2 - \omega_{z'}{}^2}, \quad \chi_{cs} = \frac{\gamma M_0\cos(\varphi_0)}{i\omega_{z'}}\sin(\theta_0).$$

Unexpectedly, the tensor $\hat{\chi}$ obtained a very simple view.

Expression (48) is the final formula in this paper for the magnetic susceptibility tensor $\hat{\chi}$ of pseudocrystal. It is essential that the magnetic susceptibility $\hat{\chi}$ has a resonance near the frequency $\omega_{\theta_0} = \omega_0\left[1 - \lambda\cos(\theta_0)\right]$, which, in turn, depends on the angle θ_0 between the vectors $\mathbf{H}_0'$ and $\mathbf{M}_0'$.

Let us also pay attention to the fact that the components χ_{xx}, χ_{xy}, χ_{yx}, and χ_{yy} of the tensor $\hat{\chi}$ have a standard construction, which can be found in works dealing with the ferromagnetic resonance theory [21, 22]. At the same time, the other tensor components are substantially different. In particular, the components χ_{zx} and χ_{zy} of the tensor $\hat{\chi}$ are periodic functions of time. This circumstance can be explained by the fact that, owing to the Einstein-de Haas effect, the pseudocrystal magnetization precesses in the ground state. The components χ_{zx} and χ_{zy} are responsible for the non-trivial magnetization dynamics of pseudocrystal (see Figs 5 and 6), which is caused by the HMF $\mathbf{H}_\omega' = (H_{1x'}, H_{1y'}, 0)\exp(i\omega t)$.

According to works [21, 22], in order to account for the dissipation processes occurring in the pseudocrystal, the frequency reduction $\omega_{\theta_0} \to \omega_{\theta_0} + i\alpha\omega_{z'}$ has to be carried out in the components of tensor (48). Again, according to works [21, 22], the intensity of absorption of the HMF energy is determined by the formula

$$Q = \frac{\omega_{z'}}{8\pi}\,\mathrm{Im}\left(\mathbf{H}_{1\omega}' \times \hat{\chi}\mathbf{H}_{1\omega}'\right). \tag{49}$$

In this work, the HMF configuration $\mathbf{H}_\omega' = (H_{1x'}, 0, 0)\exp(i\omega_{z'}t)$ is preemptive. In this case,
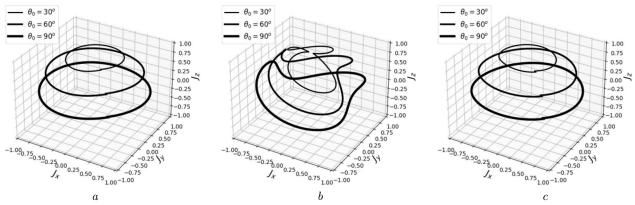
Fig. 5. Motion paths of the relative magnetization vector **J** for various values of the parameter $\Delta\bar{\omega} = -0.1$ (*a*), 0 (*b*), and 0.1 (*c*); $\overline{\omega}_1 = 0.0075$. The selected set of parameter values $\lambda = = 0.25$, $\alpha = 0.01$, $\phi_0 = 0$, and $\varphi_1 = 45°$ satisfies conditions (41)
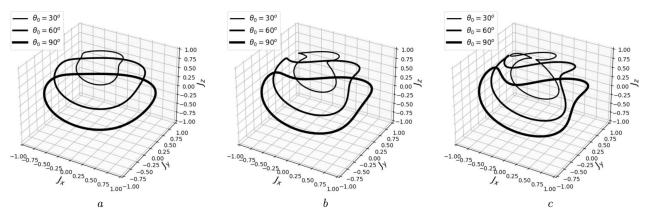

Fig. 6. Motion paths of the relative magnetization vector **J** for various values of the parameter $\overline{\omega}_1 = 0.0025$ (*a*), 0.005 (*b*), and 0.0075 (*c*) under the resonance condition ($\overline{\Delta\omega} = 0$). The selected set of parameter values $\lambda = 0.25$, $\alpha = 0.01$, $\phi_0 = 0$, and $\varphi_1 = 45°$ satisfies conditions (41)

formula (49) takes the simple form

$$Q = \frac{\omega_{z'}}{8\pi}\left[\gamma M_0 \frac{\alpha\omega_{z'}\Delta_+}{\Delta_-{}^2 + \Delta_0{}^2}\cos(\theta_0)\right]H_1{}^2, \tag{50}$$

where $\Delta_\pm = \omega_{\theta_0}{}^2 \pm (1+\alpha^2)\omega_{z'}{}^2$ and $\Delta_0 = 2\alpha\omega_{z'}\omega_{\theta_0}$.

Figure 7 demonstrates the dependences $F = = F(\theta_0, \omega)$ of the form factor of the intensity of absorption of the HMF $\mathbf{H}_{1\omega}$ energy,

$$F = 8\pi\frac{Q(\omega, \theta_0)}{\gamma M_0 H_1{}^2}, \tag{51}$$

on the main parameters of the problem. The resonance frequency at which intensive absorption of the HMF $\mathbf{H}_{1\omega}$ energy takes place is determined from the extremum condition for the function $F = F(\theta_0, \omega)$; it

looks like

$$\omega_{\text{res}} = \omega_{\theta_0}\sqrt{\frac{2(1+\alpha^2)^{1/2}}{3+\alpha^2(2-\alpha^2)} + \frac{1}{3-\alpha^2}}. \tag{52}$$

From expression (52), it is clear that the damping parameter $\alpha \ll 1$ weakly affects the value of $\omega_{\text{res}} \simeq \omega_{\theta_0}$.

The dependence of the resonance frequency $\overline{\omega}_{\text{res}}$ on the polar angle θ_0 is shown in Fig. 8.

From Figs 7 and 8, one can see that, as the polar angle θ_0 grows, the resonance frequency ω_{res} increases, and the intensity of absorption of the HMF $\mathbf{H}_{1\omega}$ energy decreases.

Thus, the found dependence of the amplitude-frequency characteristic of the intensity of absorption of the HMF $\mathbf{H}_{1\omega}$ energy by the pseudocrystal on the pseudocrystal orientation in space (the variation of
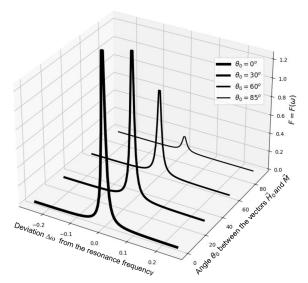
Fig. 7. Dependences $F(\theta_0, \omega)$ of the form factor F of the intensity of absorption of the HMF $\mathbf{H}_{1\omega}$ energy on the main parameters of the problem at $\lambda = 0.25$ and $\alpha = 0.01$
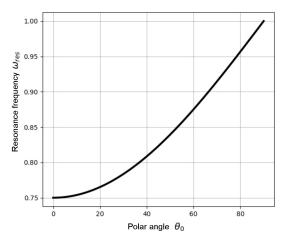

Fig. 8. Dependence of the cyclic frequency $\overline{\omega}_{\theta_0}$ on the polar angle θ_0 at $\lambda = 0.25$ and $\alpha = 0.01$

the vector $\mathbf{H}_0'$ orientation provided the fixed orientation of the vector $\mathbf{M}_0'$; see Fig. 3) can be used as a basis when developing a ferromagnetic gyroscope.

5. Conclusions

It has been shown that an FQD encapsulated in a nanocontainer whose characteristic sizes are several tens times larger than the characteristic size of the FQD can be used as a sensitive element in a ferromagnetic gyroscope.

The ferromagnetic gyroscope itself is constructed as a three-dimensional periodic layered structure (the

artificial layered crystal, the pseudocrystal) of sensitive elements (see Figs 1 and 3). This structure is rigidly fixed on a moving platform. The whole system is embedded into an external two-component magnetic field $\mathbf{H} = (H_\omega, 0, H_0)$. The static vector of the magnetic field strength $\mathbf{H}_0$ is chosen to be directed strictly perpendicularly to the pseudocrystal base, and the dynamic vector $\mathbf{H}_\omega = \mathbf{H}_1 \cos(\omega_z t)$ is directed perpendicularly to the pseudocrystal lateral face.

Before using the ferromagnetic gyroscope, the monodomain magnetic moments of the FQDs $\mathbf{m}$ must be oriented along the vector $\mathbf{H}_0$ by means of an external magnetic pulse.

Due to the law of angular momentum conservation, $\mathbf{L} = $ const, the ferromagnetic gyroscope maintains the fixed direction of the magnetization $\mathbf{M}_0$ irrespective of whether the vector $\mathbf{H}_0$ oriented perpendicularly to the moving platform changes its direction. In this case, a variation in the relative orientation of the vectors $\mathbf{M}_0$ and $\mathbf{H}_0$ is accompanied by a change in the amplitude-frequency characteristic of the intensity of the HMF energy absorption. Its spectral analysis makes it possible to obtain information about changes in the orientation of the moving platform and generate required control signals.

Note that, formally,the structure of the spectrum of absorption of the HMF energy by the FQD is similar to that available in ferromagnetic resonance studies. This fact allows the experience of radio spectroscopy to be applied when developing ferromagnetic gyroscopes with nanosized sensitive elements.

It is essential that the proposed model of ferromagnetic gyroscope includes no mechanical components. This feature of the model can increase the reliability of the construction and bring the sensitivity of ferromagnetic gyroscopes to the level achieved in radio spectroscopy.

The number of sensitive elements in the ferromagnetic gyroscope is determined by the requirements for the intensity of the HMF energy absorption by the FQD. In turn, this parameter depends on the sensitivity of the radio spectrometer that is used for the spectral analysis.

APPENDIX.
Mechanism of quantum levitation
of a ferromagnetic quantum dot

The FQD is a quasi-classical object that preserves its quantum-mechanical properties. Therefore, the dynamics of an FQD

in a nanocontainer can be considered using the quantum-mechanical methods. Since the FQD volume is much smaller than the nanocontainer one and the FQD cannot go beyond the nanocontainer boundaries, we will below consider an FQD in the framework of the model of a material point located in a deep potential well characterized by the radius r_0,

$$W = \begin{cases} \infty & \text{if } r > r_0, \\ 0 & \text{if } r \leqslant r_0, \end{cases} \tag{53}$$

where r is the radial coordinate of the FQD in the nanocontainer.

Potential energy (53) within the nanocontainer brings about the stationary radial Schrödinger equation $\hat{H}R(r) = ER(r)$ supplemented with the boundary condition $R(r \geqslant r_0) = 0$. Its specific form looks like [20]

$$\frac{d^2R}{dr^2} + \frac{2}{r}\frac{dR}{dr} + \left[k^2 - \frac{l(l+1)}{r^2}\right]R = 0, \tag{54}$$

where $k^2 = \frac{2m_0E}{\hbar^2}$, $l = 0, 1, 2, 3, \dots$ is the orbital quantum number, E is the FQD energy, and $R = R(r)$ is the radial part of the FQD wave function, which satisfies the normalization condition

$$\int_0^\infty R(r)^2 r^2 dr = 1. \tag{55}$$

By substituting the variable $\rho = kr$, Eq. (55) is reduced to the Bessel equation

$$\frac{d^2R}{d\rho^2} + \frac{2}{\rho}\frac{dR}{d\rho} + \left[1 - \frac{l(l+1)}{\rho^2}\right]R = 0, \quad R = R(\rho). \tag{56}$$

Of two solutions of Eq. (56), finite at $\rho \leqslant 0$ is the spherical Bessel function [27]
$$R = C_j j_l(\rho), \quad j_l = \sqrt{\frac{\pi}{2\rho}} J_{l+1/2}(\rho), \tag{57}$$

where C_j are integration constants whose values are determined from normalization conditions, and $J_{l+1/2}$ is the Bessel function of half-integer order. The normalized radial wave functions of the FQD have the following form:

$$R_l = 2k j_l(kr) = \sqrt{\frac{2\pi k}{r}} J_{l+1/2}(kr). \tag{58}$$

According to the properties of the function $j_l = j_l(kr)$ [27], the FQD wave function at the center of nanocontainer can be approximated by the expression

$$R_l \approx \frac{2k^{l+1}}{(2l+1)!!} r^l. \tag{59}$$

At $k\rho \geqslant 0$, the wave function equals zero since the FQD cannot be located outside the nanocontainer. From the continuity condition for the wave function at $k\rho = r_0$, we find the quantization condition for the FQD energy in the nanocontainer,
$$j_l(kr_0) = 0. \tag{60}$$

By denoting the roots of the spherical Bessel function as x_{nl}, where $n = 1, 2, 3, \dots$ is the principal quantum number, we obtain from Eq. (60) discrete values of the FQD energy,

$$k \to k_{nl} = \frac{x_{nl}}{r_0}, \quad E_{nl} = \frac{\hbar^2 x_{nl}^2}{2m_0 r_0}. \tag{61}$$

Here, from the entire set of the FQD quantum states in the nanocontainer, we are interested in the ground state, which corresponds to the quantum numbers n the spherical Bessel function. Therefore, in the ground state, the FQD has the finite energy

$$E_{10} = \frac{\hbar^2}{2m_0 r_0}\, 6.283 \neq 0, \tag{62}$$

and its wave function (58) has a maximum at the center of nanocontainer and monotonically vanishes toward the nanocontainer boundary. Such a behavior means that the FQD is most likely located at the center of nanocontainer, i.e., the FQD is in the quantum levitation state (a state without any contact with the elements of external environment).

As a result, an FQD consisting of iron atoms and having a characteristic size of $R = 1$ nm, when being placed in a container with a characteristic size of $r_0 = 10$ nm, has the following energy in the ground state:
$$E_{10} = \hbar\omega_{10}, \quad \omega_{10} = 3 \times 10^4 \text{ s}^{-1}. \tag{63}$$

Since this work has a qualitative and schematic character, the results obtained in this Appendix can be considered as quite satisfactory.

1. O.W. Richardson. A mechanical effect accompanying magnetization. *Phys. Rev. Ser. I* **26**, 248 (1908).
2. A. Einstein, W.J. de Haas. Experimenteller Nachweis der Ampereschen Molekularstrome *Deut. Physik. Gesellsch. Verhandl.* **17**, 152 (1915).
3. A. Einstein, W.J. de Haas. Experimental proof of the existence of Ampere's molecular currents. *Koninkl. Akad. Wetensch. Amsterdam* **18**, 696 (1915).
4. L.A. Levin. On the possibility of creating a cryogenic ferromagnetic gyroscope. *Zh. Tekhn. Fiz.* **66**, No. 4, 192 (1996) (in Russian).
5. P. Fadeev, Ch. Timberlake, Tao Wang, A. Vinante, Y.B. Band, D. Budker, A.O. Sushkov, H. Ulbricht, D.F. Jackson Kimba. Ferromagnetic gyroscopes for tests of fundamental physics. *arXiv:2010.08731v1 [quant-ph]*.
6. S.J. Barnett. On magnetization by angular acceleration. *Science* **30**, 413 (1908).
7. S.J. Barnett. Magnetization by rotation. *Phys. Rev.* **6**, 239 (1915).
8. S.J. Barnett. Gyromagnetic and electron-inertia effects. *Rev. Mod. Phys.* **7**, 129 (1935).
9. L.D. Landau, E.M. Lifshits, *Electrodynamics of Continuous Media* (Pergamon Press, 1984).
10. S.V. Vonsovsky. *Magnetism* (Wiley, 1974).
11. S.P. Gubin, Yu.A. Koksharov, G.B. Khomutov, G.Yu. Yurkov. Magnetic nanoparticles: Methods of preparation, structure and properties. *Adv. Chem.* **74**, 6 (2005).
12. S.V. Terekhov, V.N. Varyukhin. *Physics of Nanoobjects* (DonNU, 2013) (in Russian).
13. Yu.M. Poplavko, O.V. Borysov, I.P. Golubeva, Yu.V. Didenko. *Magnets in Electronics* (KPI, 2021) (in Ukrainian).
14. O.I. Tovstolytkin, M.O. Borovyi, V.V. Kurylyuk, Yu.A. Kunitskyi. *Physical Foundations of Spintronics* (ToV "Nilan-LTD", 2014) (in Ukrainian).

15. S.A. Sokolsky. The influence of interparticle interaction in an ensemble of stationary superparamagnetic ferroparticles on the statistical, magnetic and thermodynamic properties of the system. *Comp. Cont. Mech.* **14**, 264 (2021) (in Ukrainian).

16. C. Zhang, H. Yuan, Z. Tang, W. Quan, J.C. Fang. Inertial rotation measurement with atomic spins: From angular momentum conservation to quantum phase theory. *Appl. Phys. Rev.* **3**, 041305 (2016).

17. J. Gieseler, A. Kabcenell, E. Rosenfeld, J.D. Schaefer, A. Sara, M.J.A. Schuetz, C. Gonzalez-Ballestero, C.C. Rusconi, O. Romero-Isart, M.D. Lukin. Single-spin magnetomechanics with levitated micromagnets. *Phys. Rev. Lett.* **124**, 163604 (2020).

18. A. Vinante, P. Falferi, G. Gasbarri, A. Setter, C. Timberlake, H. Ulbricht. Ultralow mechanical damping with Meissner-levitated ferromagnetic microparticles. *Phys. Rev. Appl.* **13**, 064027 (2020).

19. P. Huillery, T. Delord, L. Nicolas, M. Van Den Bossche, M. Perdriat, G. Hetet. Spin mechanics with levitating ferromagnetic particles. *Phys. Rev. B* **101**, 134415 (2020).

20. L.D. Landau, E.M. Lifshitz. *Quantum Mechanics. Non-Relativistic Theory* (Pergamon Press, 1981).

21. A.G. Gurevich. *Magnetic Resonance in Ferrites and Antiferromagnets* (Nauka, 1973) (in Russian).

22. V.G. Shavrov, V.I. Shcheglov. *Feromagnetic Resonance under Conditions of Orientational Transition* (Nauka, 2018) (in Russian).

23. J. Smit, H.P.J. Wijn. *Advances in Electronics and Electron Physics VI* (Academic Press, 1954).

24. J. Smit, H.G. Beljers. Ferromagnetic resonance absorption in $BaFe_{12}O_{19}$, a highly anisotropic crystal. *Philips Res. Rep.* **10**, 113 (1955).

25. H. Suhl. Ferromagnetic resonance in nickel ferrite between one and two kilomegacycles. *Phys. Rev.* **97**, 555 (1955).

26. G.V. Skrotskii, T.V. Kurbatov. Phenomenological theory of ferromagnetic resonance. In *Ferromagnetic Resonance. Edited by S.V. Vonsovskii* (Nauka, 1961) (in Russian).

27. J. Campe de Ferrier, R. Campbell, G. Petiot, T. Vogel. *Functions of Mathematical Physics: Reference Guide. Translation from French by N.Ya. Vilenkin* (Fizmatgiz, 1963) (in Russian).

М.М. Чепілко, С.О. Пономаренко

ФІЗИЧНІ ОСНОВИ ФЕРОМАГНІТНОГО ГІРОСКОПА З НАНОРОЗМІРНИМИ ЧУТЛИВИМИ ЕЛЕМЕНТАМИ

Розглянуто фізичні основи застосування сучасних нанотехнологій для розробки нанорозмірних та енергоефективних чутливих датчиків для систем управління малогабаритних супутників. Практичний інтерес викликає створення феромагнітного гіроскопа, в ролі моделі якого пропонується використати періодичну структуру (псевдокристал) з когерентних монодоменних феромагнітних квантових точок (ФКТ), локалізованих у сферичних наноконтейнерах, де вони будуть перебувати у стані квантової левітації. Внаслідок ефекту Ейнштейна–де Гааза, ФКТ будуть мати момент імпульсу, що зберігається у часі. Для контролю за орієнтацією псевдокристала у просторі він кріпиться до рухомої платформи, розміщеної у зовнішньому двокомпонентному магнітному полі (МП). Статична компонента МП є перпендикулярною до основи псевдокристала, а динамічна – до його бічної сторони. За рахунок аналізу спектра поглинання динамічного МП, залежного від орієнтації псевдокристала у просторі, існує можливість розрахувати кутові координати його нового положення, які визначаються взаємною орієнтацією фіксованого напрямку моменту імпульсу ФКТ та вектора зовнішнього статичного МП.

К л ю ч о в і   с л о в а: нанофізика, наночастинка, феромагнітна квантова точка, левітація, гіроскоп, спін, магнетон, момент імпульсу.